

Use of the stiffness method to evaluate the improvement of the bearing capacity of soil reinforced by microgrids

Neyla Lima Carneiro Sernache^{1#} , Anderson Borghetti Soares¹ ,

Marcos Fábio Porto de Aguiar² 

Article

Keywords

Soil reinforcements
Geosynthetics
Microgrid
Plate load test

Abstract

The search for soil strength and stiffness improvement is essential in geotechnical engineering. Geosynthetic reinforcement has been considered an effective solution, as it increases the stability of geotechnical works and reduces settlement. These materials are used in works that require greater stiffness, as well as shear and tensile strength, such as foundations and retaining walls. Among geosynthetics, microgrids are used to promote the separation and reinforcement of soils. However, because it is a recently developed geosynthetic on the market, little is known about its properties in soil reinforcement structures, especially when compared with other geosynthetics with the same function, highlighting the need for more research. This research aimed to evaluate the improvement in the bearing capacity of soils reinforced with microgrids. As the results of the pressure x settlement curves did not characterise a typical physical failure behaviour, the failure was conventionally defined based on the Décourt stiffness method. Through the analysis of pressure x settlement curves, the behaviour of natural soils was compared with (i) compacted samples and (ii) compacted samples reinforced with three layers of microgrids. This demonstrated the increase in soil bearing capacity and stiffness through these improvement techniques, which was even more significant when microgrids were inserted in the compacted soil sample. The inclusion of microgrids as a reinforcing element is an effective alternative for stabilising foundations. The stiffness curves showed a tendency to stabilise without reaching zero stiffness, which, according to the Décourt method, confirms the absence of physical failure.

1. Introduction

Soils with low strength and high compressibility represent a frequent challenge in geotechnical engineering due to their inability to withstand significant loads and the risk of excessive settlements. Several techniques have been employed to improve their mechanical properties, including compaction, soil-cement mixtures, soil-fibre mixtures, and the application of polymeric materials, such as geosynthetics.

Geosynthetics are petroleum-derived products manufactured from polymers, bases, and additives. They are used in geotechnical works for various functions, including separation, filtration, drainage, and reinforcement. Their application enables excellent technical and economic efficiency while increasing the durability of structures and reducing costs using conventional materials (Palmeira, 2018).

Several studies conducted with load tests on plates have shown that reinforcing soils with geosynthetics significantly

increases their load capacity and stiffness, thereby improving their mechanical properties. Studies such as those by Adams & Collin (1997), Santos et al. (2021), and Guedes et al. (2019) have demonstrated these benefits.

Adams & Collin (1997) investigated the use of geocells and geogrids in sandy soils, analysing variables such as number of layers, spacing, type of material, and sand density. They concluded that these factors directly influenced the structural performance of reinforced soils and highlighted the need for specific adjustments to optimise results. Santos et al. (2021) also studied the use of geocells and geogrids as reinforcements in sandy soils. They observed improved soil mechanical properties, with better results obtained with geogrids, especially when the number of layers was increased. Guedes et al. (2019) compared the performance of sisal and polypropylene geogrids in reinforced soils. Both materials improved load capacity, but polypropylene showed superior performance.

#Corresponding author. E-mail address: neyla.carneiroeng@gmail.com

¹Universidade Federal do Ceará, Departamento de Engenharia Hidráulica e Ambiental, Fortaleza, CE, Brasil.

²Instituto Federal de Educação, Ciência e Tecnologia do Ceará, Departamento de Construção Civil, Fortaleza, CE, Brasil.

Submitted on December 13, 2024; Final Acceptance on September 5, 2025; Discussion open until May 31, 2026.

Editor: Renato P. Cunha 

<https://doi.org/10.28927/SR.2026.011124>



This is an Open Access article distributed under the terms of the Creative Commons Attribution license (<https://creativecommons.org/licenses/by/4.0/>), which permits unrestricted use, distribution, and reproduction in any medium, provided the original work is properly cited.

Microgrids are among the recently developed geosynthetics. They are lightweight materials used for soil separation and reinforcement, characterised by high tensile strength and static punching properties. Produced in polyester with PVC coating, they offer protection against installation damage and chemical, environmental, and biological agents (ABNT, 2013). Although some laboratory studies have explored the use of microgrids for soil reinforcement, such as those by Bessa (2022), Teles Júnior (2022) and Teles Júnior et al. (2025), scientific investigations involving microgrids remain scarce. This is the first study to evaluate, under real loading conditions, the behaviour of soils reinforced with microgrids through plate load tests. The research aims to fill the gap in understanding the performance of microgrids in the field, thereby contributing to the understanding of their effectiveness as a reinforcement material. Since the tests did not indicate physical rupture, the conventional rupture load was estimated by the Décourt (1996, 2008) method.

Failure occurs when the soil mobilises its maximum resistance, resulting in excessive deformations or collapse (Teixeira & Godoy, 1998). According to Décourt (1996, 2008), although the load test is considered the most reliable method for assessing the actual behaviour of foundations, it is common in practice for the tests not to reach physical failure or even conventional failure.

This method allows estimating two definitions of failure load by extrapolation: physical, associated with zero stiffness (i.e., infinite deformation, when the soil no longer offers additional resistance), and conventional, corresponding to a settlement equal to 10% of the width of the footing or the diameter of the pile (or 30% for bored piles). Based on correlations, the method provides a more accurate description of the load and settlement relationship, enabling the results to be interpreted using the load and stiffness graph (Décourt, 1996, 2008).

For its application, the data from the load tests are organised into load and settlement pairs, in decreasing order of load. Linear regressions are then performed between the values transformed into a logarithmic scale, starting with the last three points of the curve and progressively including more points as needed. The quality of the fit is assessed by the correlation coefficient, which should preferably be greater than 0.99. The regression equation obtained from the best fit (defined as the regression point) enables the estimation of the load associated with conventional settlements and the extrapolation of the load-settlement curve.

Stiffness is calculated as the ratio of the applied load to the settlement. Based on this relationship, regressions are performed between the logarithms of the load and stiffness, adopting the same regression point as the load & settlement curve. The resulting equation enables the construction of an extrapolated stiffness graph, which indicates whether physical rupture has occurred.

Décourt (1996, 2008) states that physical rupture occurs when stiffness (R) reaches zero, which is only observed in

specific situations, such as displacement piles and soil-pile lateral friction. In direct foundations, such as footings and plates, the load versus stiffness curve tends to a sub-horizontal asymptote that does not intercept the abscissa axis, indicating that stiffness is progressively reduced, but without reaching zero. Physical rupture would only be approximated for deformations of the order of magnitude of several times the width of the footing, a condition of no practical interest.

2. Materials and methods

The soil analysed in this research was collected in the Experimental Field of Geotechnics and Foundations (CECEF) of the Federal University of Ceará (UFC) in Fortaleza, State of Ceará, Brazil. Three samples were taken for geotechnical characterisation and compaction tests: one at the location chosen for the load test in natural soil and two at a depth of 35 cm in the pits for the load tests in compacted soil and compacted soil with microgrids. The average laboratory results were used in the field trials.

The characterisation tests included particle size analysis, as per NBR 7181 (ABNT, 2016e); consistency limits, as outlined in NBR 6459 (ABNT, 2016c) and NBR 7180 (ABNT, 2016d); and particle density, as specified in NBR 6458 (ABNT, 2016b). Compaction tests were also conducted by the guidelines of NBR 6457 (ABNT, 2016a) and NBR 7182 (ABNT, 2016f). The compaction tests were performed using standard Proctor energy, with soil reused.

The geosynthetic used in this study was a microgrid, manufactured and distributed by Maccaferri under the trade name MacGrid Net. According to Maccaferri's Catalogue of Technical Specifications (Maccaferri, 2019), the microgrid has a longitudinal tensile strength of 45 kN/m and a maximum elongation of 15%. The mesh opening is 2 mm × 1,5 mm. Figure 1 illustrates the microgrid used in the tests.

The experimental program consisted of three load tests performed under different conditions: (A) compacted soil in a 75-cm-deep pit, (B) compacted soil with three layers of

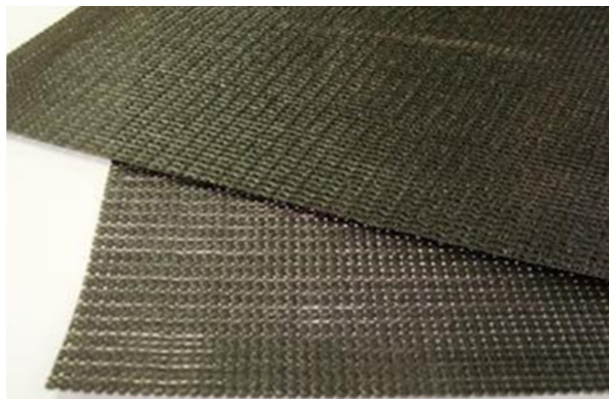


Figure 1. Microgrid (MacGrid Net – Maccaferri).

microgrid in a 75-cm-deep pit, and (C) natural soil (without reinforcement). Figure 2 illustrates the upper view of the model pits, while Figures 3 and 4 show the details of the profile configurations for each model.

The elements of the models are the spacing between the foundation and the top reinforcing layer (u), the height of the compacted layer (a_c), the vertical spacing between the reinforcing layers (h), the total number of reinforcing layers (N), the depth from the soil surface to the reinforcing layer n (Z_n), the total depth of the reinforcement (d), the length of reinforcement and pit (L), the depth of the foundation (D_f), and the total height of the pit (H). These elements define the geometry and structural characteristics used in the model tests.

The height of the pit (H) was defined, considering the concept of stress bulb, which, in circular plates, is equivalent

to $2B$, where B is the width or diameter of the spread footing. At this depth, approximately 90% of the stresses are dissipated (Teixeira & Godoy, 1998), which corroborates the recommendations of NBR 6489 (ABNT, 2019), where stresses exceeding 10% of the allowable stress for direct foundation projects are considered representative. The height of the compacted layers (a_c) was set at 15 cm, as recommended by Sousa Pinto (2006), who suggests thicknesses between 15 and 20 cm due to the decreased efficiency of compaction equipment at greater depths.

In this study, the microgrid was placed over the entire excavation area ($80\text{ cm} \times 80\text{ cm}$) to enhance soil reinforcement. This length (L), as well as the spacing between the foundation and the upper reinforcing layer (u), the vertical spacing between the reinforcements (h), and the total depth of the reinforcement (d), were defined by the recommendations of Sharma et al. (2009). These authors studied and compared different configurations of reinforcement spacings in reinforced soil models, establishing intervals to maximise reinforcement efficiency. They recommended that the first reinforcement layer be positioned at a depth of $0.2B$ to $0.5B$ from the base of the spread footing. The vertical spacing between the reinforcement layers (h) should range from $0.2B$ to $0.5B$, the total depth of reinforcement (d) from $1.0B$ to $2.0B$, and the length of reinforcement (L) from $2.0B$ to $8.0B$.

Three reinforcement layers were used, based on the results of Adams & Collin (1997), who observed improved

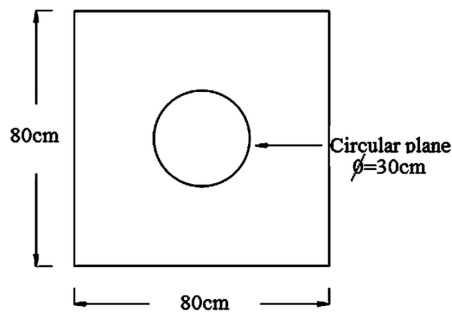


Figure 2. Upper view of models 1 and 2.

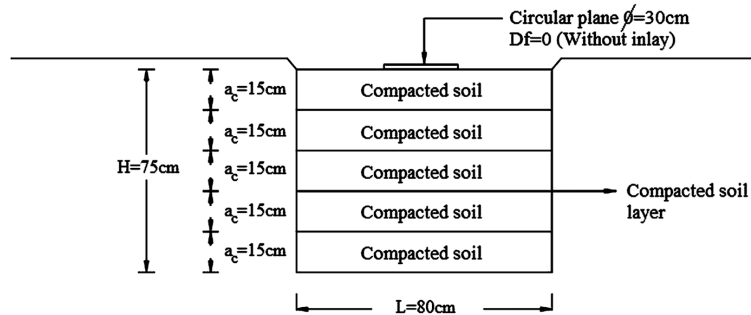


Figure 3. Model 1 - layout of the compacted soil pit.

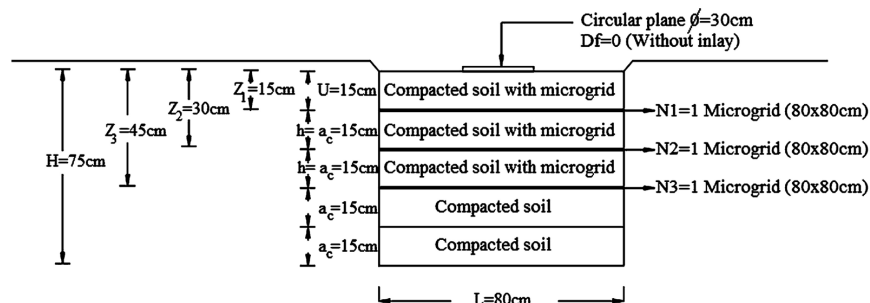


Figure 4. Model 2 - layout of the pit with compacted soil intercalated with microgrids.

load capacity results when using a reinforced soil model with three layers of geosynthetics interspersed with compacted soil.

The experimental models were implemented through excavations made with the designed dimensions (Figures 3 and 4), correcting the soil moisture to achieve compaction and homogenising it. The compaction control was performed in the field using an electronic scale, a Speedy moisture tester, and a crimping cylinder. Each soil layer was compacted at optimum moisture with a gasoline-powered percussion compactor, model Wacker BS50-2, which compacted 196.8 kg of soil per layer. The water content was checked in situ and corrected by adding water when necessary.

After homogenization, the soil was deposited in the pit, levelled, and compacted to ensure the appropriate height of the layers. The dry apparent specific mass was verified with a spiked cylinder, and the degree of compaction was required to be 95% or higher. Once the desired degree of compaction was reached, the soil was recompacted, and the process was repeated in layers until the pit was filled.

In model 2, the same execution process was followed, but the microgrids were included.

Load tests were performed using a 30 cm diameter circular plate. Loads were applied quickly and progressively, in uniform increments of 160 kPa until reaching 1,600.0 kPa. The test consisted of ten loading stages and five unloading stages, following the procedures established by NBR 6489 (ABNT, 2019). Figure 5 shows records of the three test conditions, including the assembly of the model with microgrids.

3. Results and discussions

The particle size distribution curves (Figure 6) showed that the soil was sandy and homogeneous, containing approximately 10% of fines. According to the Unified Soil Classification System (USCS), the three samples were classified as SW, presenting non-uniformity coefficients (*NUC*) of 4.95, 5.0, and 5.91 and curvature coefficients (*CC*) of 2.05, 2.05, and



Figure 5. Load tests: (a) natural soil; (b) compacted soil; (c) compacted soil with microgrid.

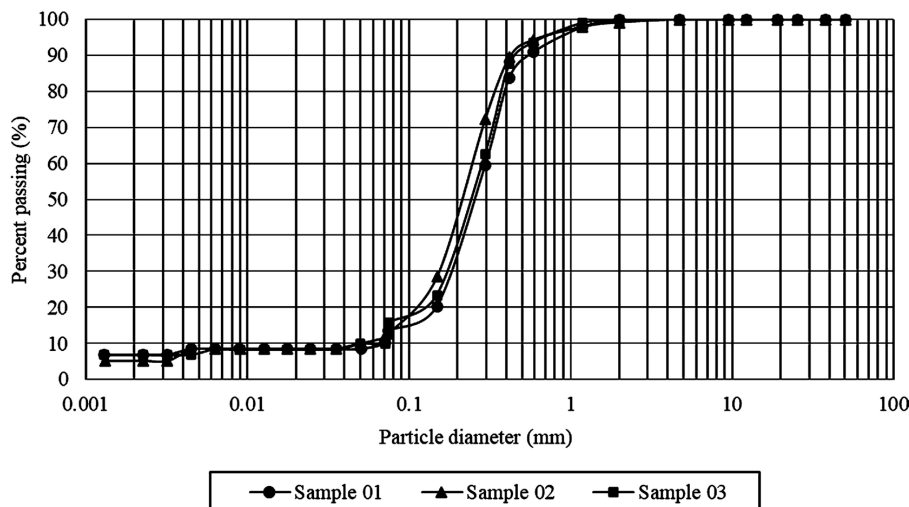


Figure 6. Particle size distribution.

2.4, respectively. These values characterise a well-graded, non-uniform sand. Compaction tests revealed an optimal water content (w) of 9.3% and a maximum dry unit weight of 18.37 kN/m^3 (Figure 7).

Figure 8 presents the results of the load tests conducted under three different conditions: natural soil, compacted soil, and compacted soil with three layers of microgrids, as represented by the pressure-settlement curve, up to a pressure of 1,600 kPa.

The maximum settlement in the natural soil was 7.71 mm. In compacted soil, settlement decreased to 7.16 mm, corresponding to a decrease of 7.13% in natural soil. In the compacted soil with a microgrid, the settlement was 6.01 mm, representing a 22% reduction compared to natural

soil and a 16.06% reduction compared to compacted soil without a microgrid.

As shown in Figure 8, no evidence of physical failure was observed. To determine the conventional failure pressure and further confirm the absence of physical failure in shallow foundations, the extrapolation method of Décourt (1996, 2008) was applied, using the data obtained in the load tests.

Figures 9 to 11 illustrate the results of applying Décourt's (1996, 2008) method to the field data. They present the best-fit regression curves and their respective equations, enabling the estimation of the soil's behaviour under various loading conditions.

Figure 9 shows that the conventional failure of the natural soil occurred at a pressure of 3,740 kPa, a pressure

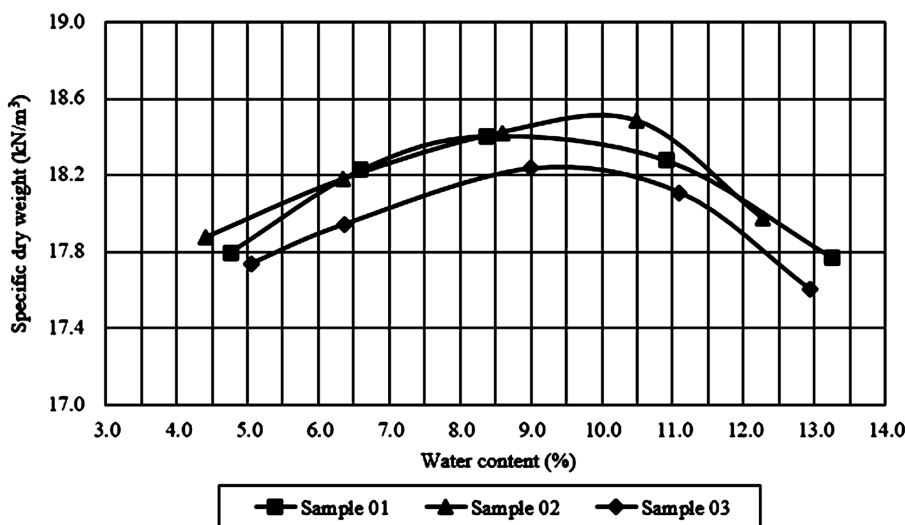


Figure 7. Soil compaction curves.

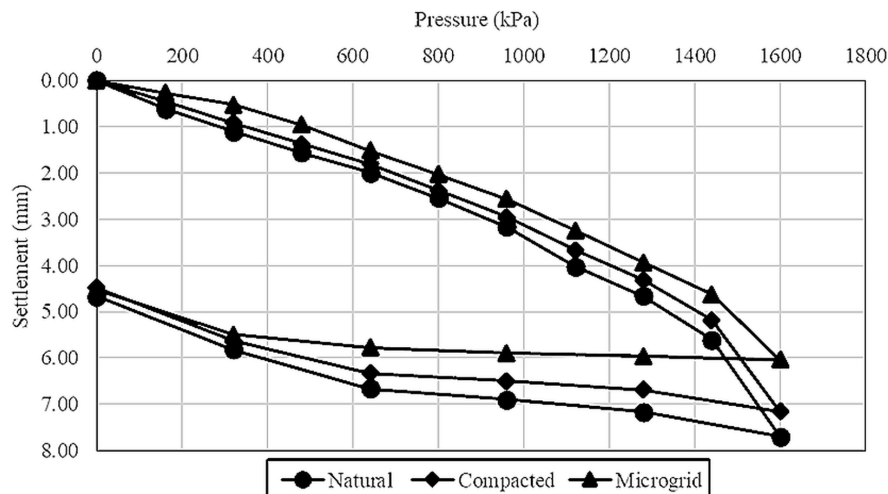


Figure 8. Pressure x settlement curve for natural soil, compacted soil, and compacted soil with microgrid.

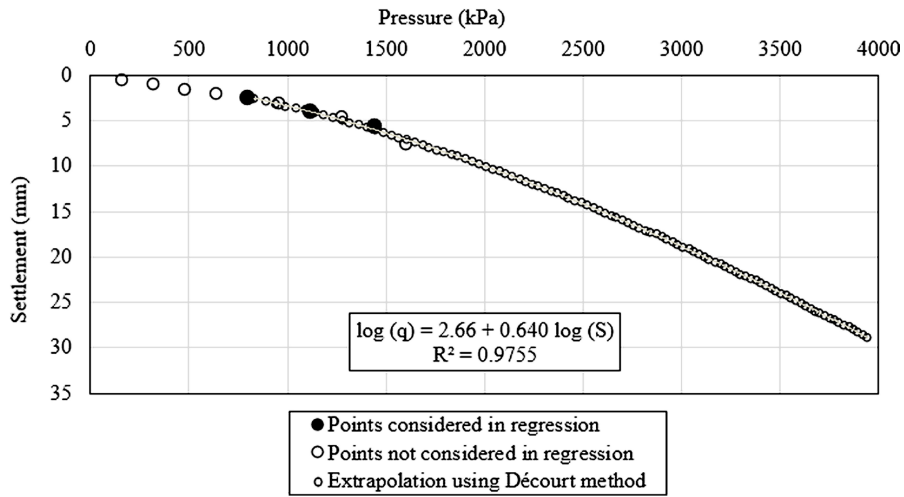


Figure 9. Pressure x settlement curve using Décourt's method for natural soil.

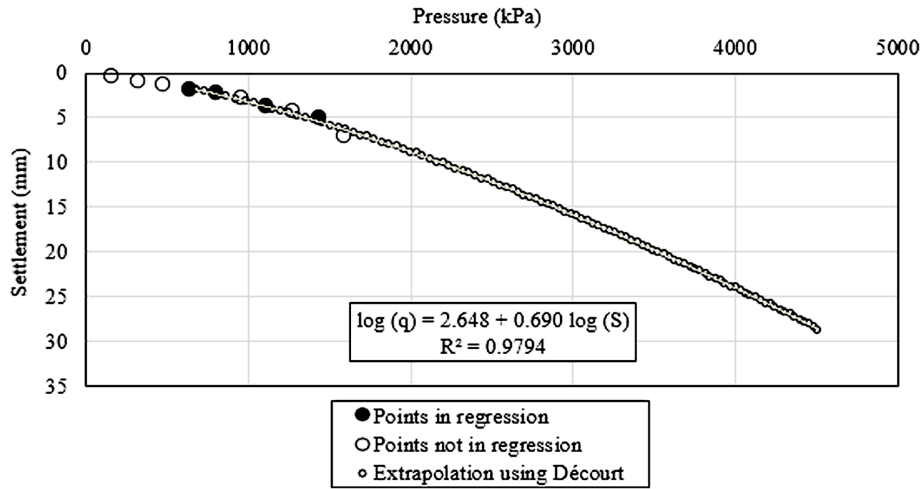


Figure 10. Pressure x settlement curve using Décourt's method for compacted soil.

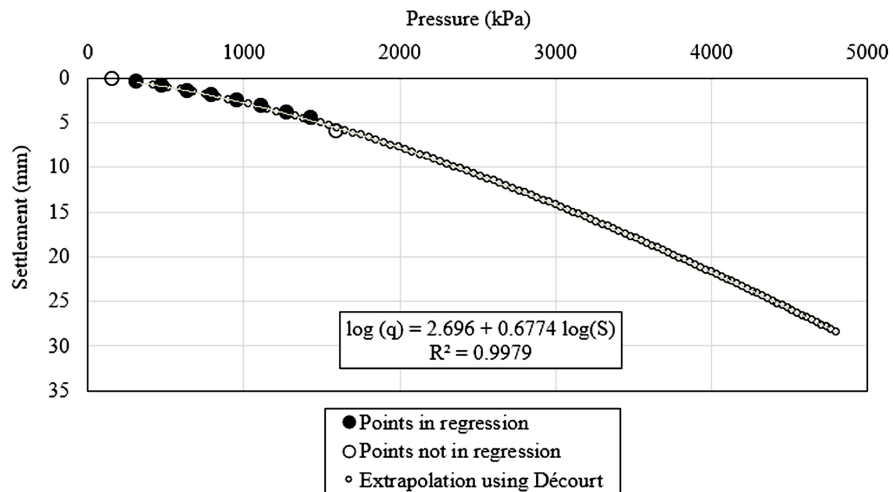


Figure 11. Pressure x settlement curve using Décourt's method for compacted soil with microgrid.

that corresponds to the settlement of 26.58 mm, which according to Décourt (1999) is equivalent to 10% of the equivalent width (B_{eq}), where $(B_{eq}) = A^{0.5}$, A being its spread footing area. Figures 10 and 11 show that the conventional failure pressure was 4,280 kPa for compacted soil and 4,577 kPa for compacted soil with microgrids, respectively. The results indicate that soil compaction increased the failure pressure by 14.43% to the natural soil. The combination of compaction with the microgrid proved even more effective, with a 22.38% increase in failure pressure.

The conventional failure pressure of the natural soil was used to compare the settlements. The settlement in the natural soil was 26.58 mm, while in the compacted soil, it was 21.81 mm, representing an 18% reduction. With the microgrid, the settlement was 19.71 mm, representing a 26% reduction compared to natural soil and a 10% reduction compared to compacted soil. These soil improvement techniques increased the stiffness of the soil, reducing settlements and, consequently, improving its bearing capacity. Thus, it can be seen that with the use of improvement techniques, the soil becomes more rigid and deforms less than natural soil for the same applied pressure, thus increasing its bearing capacity, which corroborates the improvements in mechanical properties observed by Teles Júnior (2022) in his triaxial tests with compacted soil and soil compacted with microgrids.

Figure 11 shows that during the assembly of the linear correlations between $\log q$ and $\log S$, where q represents the applied pressure (kPa) and S the measured settlement (mm), practically all points of the load test were used in the correlations without requiring additional adjustments to optimise the correlation coefficient. The compacted soil with microgrid generated a graph with field data that was more closely adjusted to the statistically generated curve than those of the load test in natural soil and the load test in compacted soil, as verified by the highest R^2 value of 0.9979.

Figures 12 to 14 present the results of the pressure curves versus stiffness (R), with the data extrapolated using the Décourt (1996, 2008) method. It can be observed that as the load increases, stiffness decreases, with a clear tendency to approach a sub-horizontal asymptote without intersecting the x-axis. This behaviour confirms that there is no physical failure (represented by the point of zero stiffness), which corroborates Décourt's theory.

Figure 15 shows the pressure-stiffness curves from the three plate load tests. The compacted soil with microgrids exhibited greater stiffness when subjected to loads. It was observed that improvement techniques increased stiffness for the same stress level. Considering the conventional failure pressure of the natural soil, the stiffness was 140.6 kPa/mm. In compacted soil, the stiffness increased to 171.3 kPa/mm, representing a 21.83% increase in stiffness. The microgrid compaction combination was even more effective, reaching 189.7 kPa/mm, representing an increase of 34.92% compared to natural soil and 10.74% compared to compacted soil.

The small gain resulting from compaction may be related to the low compressibility of the sandy soil tested, which presented high rigidity in its natural state, limiting the effects of compaction observed in the tests.

The modulus of elasticity (E) is crucial for understanding the mechanical behaviour of soils. In this study, the variation of this parameter was analysed under different applied pressures based on the theory of elasticity. Considering the stratigraphy obtained in the SPT test, the homogeneous medium hypothesis was adopted since the soil in the test layer and the area of influence of the stress bulb were the same. Using a Poisson coefficient of 0.3, typical for sands, Figure 16 was constructed, which shows the relationship between the modulus of elasticity (E) and the applied pressures, evaluating the influence of stress on soil deformability.

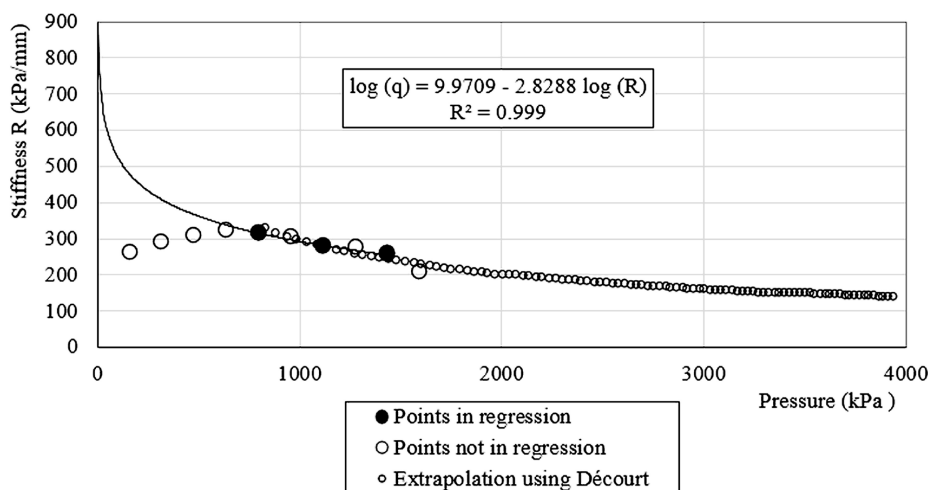


Figure 12. Pressure-stiffness curve for natural soil.

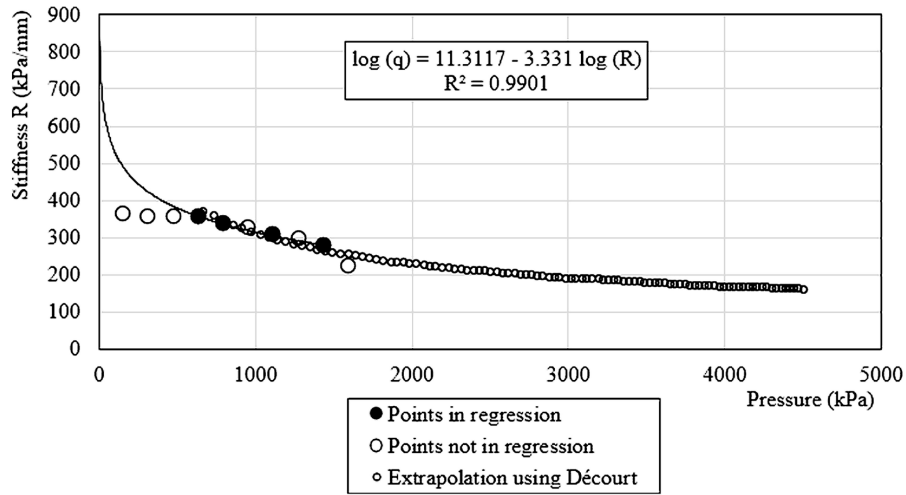


Figure 13. Pressure-stiffness curve for compacted soil.

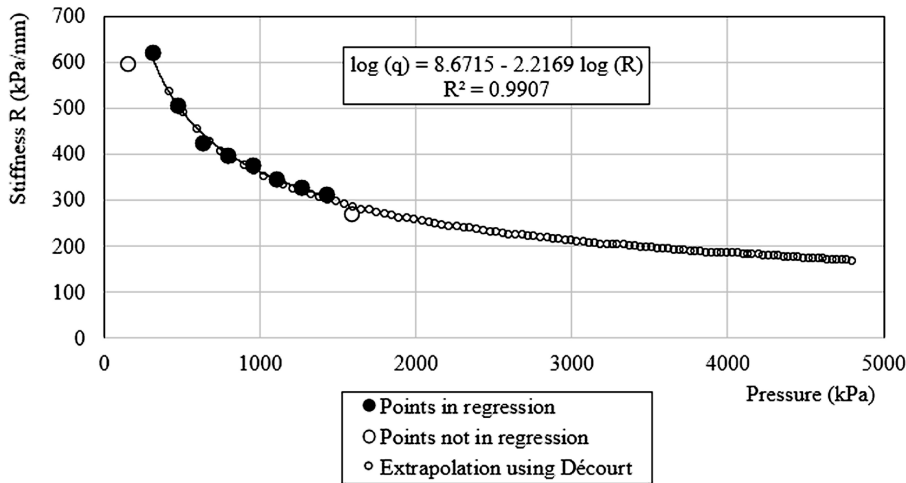


Figure 14. Pressure-stiffness curve for compacted soil with a microgrid.

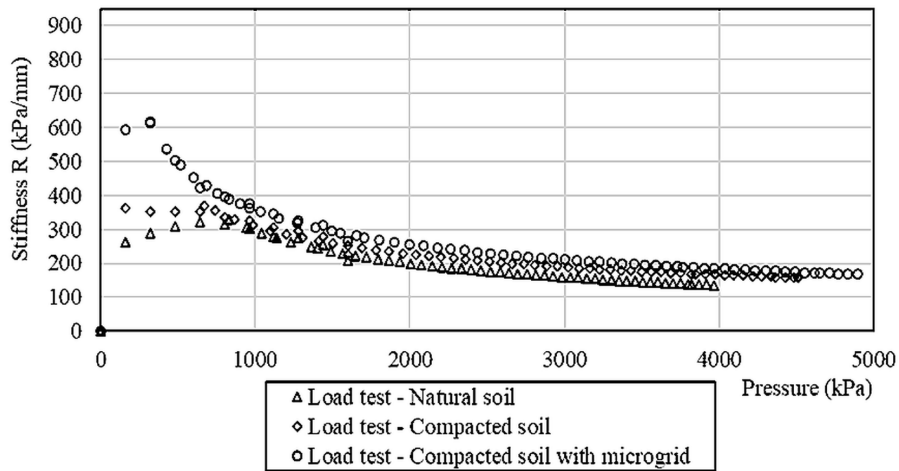


Figure 15. Pressure-stiffness curves from load tests for natural soil, compacted soil, and compacted soil with microgrid, using Décourt's method.

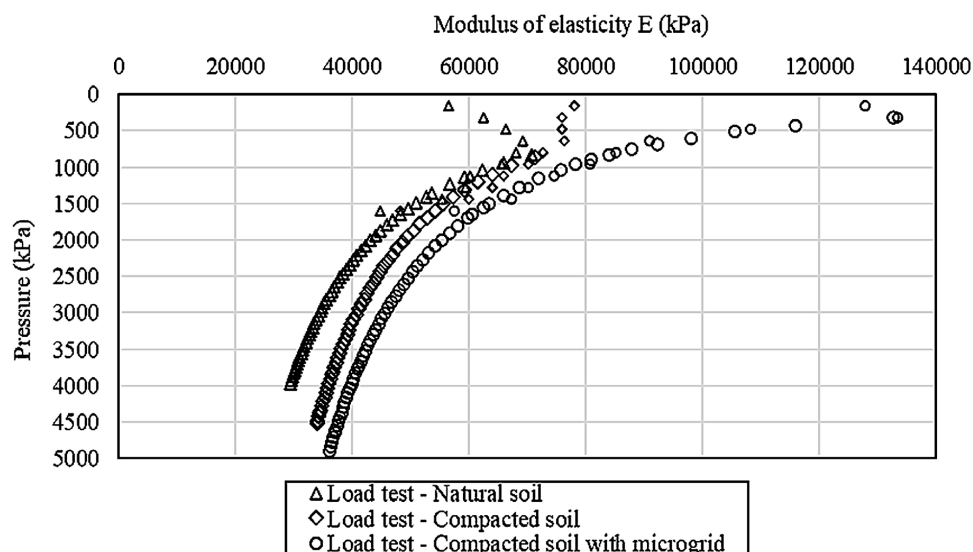


Figure 16. Load test curves (modulus of elasticity \times pressure) for natural soil, compacted soil, and compacted soil with microgrid.

Figure 16 shows that the modulus of elasticity values of the natural soil are consistent, considering the values presented by Teixeira & Godoy (1998) for medium-compact sand as a reference. Regarding the improved soils, it was not possible to compare them with the literature, as no data are available; however, the increase is justifiable due to the application of improvement techniques. This increase corroborates the results obtained by Teles Júnior (2022), who found that the inclusion of reinforcements and the rise in the number of microgrid layers increased the drying modulus of elasticity, thereby increasing the stiffness of the analysed specimens.

The load test in compacted soil revealed a modulus of elasticity greater than that of natural soil, indicating that compaction increases stiffness and resistance to deformation under pressure, proving its effectiveness in improving soil stiffness. Adding microgrids to the compacted soil initially increases the modulus of elasticity, especially at lower pressures, suggesting that the microgrids act as additional reinforcement, limiting lateral deformation and more evenly distributing stresses. However, at higher pressures, the further effect of the microgrids decreases, and the modulus of elasticity approaches that of compacted soil alone, suggesting a limitation in the reinforcement capacity of the microgrid or the exhaustion of the confinement effect provided by the microgrid.

It is also observed that, as the load increases, the modulus of elasticity varies, demonstrating non-linear behaviour. In practice, this is a fact observed in soils, even at small loading levels, as the soil often does not behave fully elastically, and the deformations do not return to zero.

4. Conclusions

This study evaluated the improvement in the mechanical behaviour of a natural sandy soil, considering a compacted sample and a compacted sample with three layers of microgrids, through plate load tests. The results confirmed that using microgrids as a reinforcement material for compacted soils effectively improves the bearing capacity and stiffness of sandy soils. Unlike natural soil, load tests showed that compaction reduced settlements and increased soil failure stress, with even more significant gains when microgrids were inserted.

When analysing the modulus of elasticity (E) with the different pressures applied in the three tests performed, it was found that using soil improvement techniques increased the modulus of elasticity, with the most significant increase observed when microgrids were included. However, at higher pressures, the additional effect of the microgrids decreases, and the modulus of elasticity approaches just the compacted soil, suggesting a limitation in the effectiveness of the microgrid in its reinforcement capacity or the exhaustion of the confinement effect on the microgrid.

It was found that as the load increases, the modulus of elasticity varies, presenting non-linear behaviour. This reflects the reality of the soils, even at small loading levels, as they do not always behave fully elastically since the deformations do not completely return to zero.

It was observed in the stiffness graphs that as the load increased in all the performed tests, the stiffness decreased, with a clear tendency to approach a horizontal asymptote without touching the abscissa axis, proving that no physical

rupture occurs (represented by the zero-stiffness point) in direct load tests, which corroborates Décourt's theory (Décourt, 1996, 2008).

In addition, the study reinforces the importance of using field tests for soil improvement techniques under more realistic conditions, expanding the possibilities of applying microgrids in geotechnical engineering works. These results pave the way for new research addressing microgrid behaviour in different soil conditions and loads.

Declaration of interest

The authors declare that they have no conflicts of interest. All co-authors noted and affirmed the paper's content, and there is no financial interest to be reported.

Authors' contributions

Neyla Lima Carneiro Sernache: conceptualization, funding acquisition, research, data curation, methodology, software, visualization, writing – original draft. Anderson Borghetti Soares: conceptualization, investigation, formal analysis, data curation, methodology, supervision, validation, writing – review and editing. Marcos Fábio Porto de Aguiar: acquisition of material for tests, methodology, supervision, validation.

Data availability

The datasets generated and analysed during the current study are available upon request from the corresponding author.

Declaration of use of generative artificial intelligence

This work was not prepared with the aid of generative artificial intelligence (GenAI).

List of symbols and abbreviations

a_c	Height of compacted layer
d	Total depth of reinforcement
h	Vertical spacing between reinforcing layers
q	Applied pressure
u	Spacing between the foundation and top reinforcement layer
w	Water Content
A	Area
B	Spread footing width
B_{eq}	Equivalent spread footing width
CC	Coefficient of curvature
CECEF	Experimental Field of Geotechnics and Foundations
D_f	Foundation depth
E	Modulus of elasticity

H	Total height of the pit
L	Length of reinforcement and pit
N	Total number of reinforcing layers
NUC	Non-uniformity coefficients
R	Stiffness
R^2	Correlation coefficient
S	Settlement
UFC	Federal University of Ceará
USCS	Unified Soil Classification System
$Z_{(n)}$	Depth from the ground surface to the reinforcement layer n

References

- ABNT NBR ISO 10.318. (2013). *Geossintéticos: termos e definições*. Associação Brasileira de Normas Técnicas, Rio de Janeiro (in Portuguese).
- ABNT NBR 6457. (2016a). *Amostras de solo: preparação para ensaios de compactação e ensaios de caracterização*. Associação Brasileira de Normas Técnicas, Rio de Janeiro (in Portuguese).
- ABNT NBR 6458. (2016b). *Grãos de pedregulho retidos na peneira de abertura 4,8 mm: determinação da massa específica, da massa específica aparente e da absorção de água*. Associação Brasileira de Normas Técnicas, Rio de Janeiro (in Portuguese).
- ABNT NBR 6459. (2016c). *Solo: determinação do limite de liquidez*. Associação Brasileira de Normas Técnicas, Rio de Janeiro (in Portuguese).
- ABNT NBR 7180. (2016d). *Solo: determinação do limite de plasticidade*. Associação Brasileira de Normas Técnicas, Rio de Janeiro, RJ (in Portuguese).
- ABNT NBR 7181. (2016e). *Solo: análise granulométrica*. Associação Brasileira de Normas Técnicas, Rio de Janeiro, RJ (in Portuguese).
- ABNT NBR 7182. (2016f). *Solo: ensaio de compactação*. Associação Brasileira de Normas Técnicas, Rio de Janeiro, RJ (in Portuguese).
- ABNT NBR 6489. (2019). *Solo: prova de carga estática em fundação direta*. Associação Brasileira de Normas Técnicas, Rio de Janeiro, RJ (in Portuguese).
- Adams, M.T., & Collin, J.G. (1997). Large-scale model spread footing load tests on geosynthetic-reinforced soil foundations. *Journal of Geotechnical and Geoenvironmental Engineering*, 123(1), 66-72. [https://doi.org/10.1061/\(ASCE\)1090-0241\(1997\)123:1\(66\)](https://doi.org/10.1061/(ASCE)1090-0241(1997)123:1(66)).
- Bessa, A.K.S. (2022). *Estudo dos parâmetros de resistência da interface entre solo-geossintético por meio de cisalhamento direto* [Master's dissertation, Federal University of Ceará]. Federal University of Ceará's repository (in Portuguese). Retrieved in November 9, 2024, from <https://www.repositorio.ufc.br/handle/riufc/69272>
- Décourt, L. (1996). A ruptura de fundações avaliada com base no conceito de rigidez. In *Anais do III Seminário de*



- Engenharia de Fundações Especiais e Geotecnia (SEFE)* (Vol. 1, pp. 215-224). São Paulo: ABMS (in Portuguese).
- Décourt, L. (1999). Behavior of foundations under working load conditions. In *Proceedings of the 11th Pan-American Conference on Soil Mechanics and Geotechnical Engineering* (Vol. 4, pp. 453-488), Foz do Iguaçu, PR. São Paulo: ABMS.
- Décourt, L. (2008). Provas de carga em estacas podem dizer muito mais do que têm dito. In *Anais do 6º Seminário de Engenharia de Fundações Especiais e Geotecnia (SEFE)* (Vol. 1). São Paulo: ABMS.
- Guedes, E.S.R., Rocha, E.P.L., Moura, G.J., & Menezes, J.H.F. (2019). Avaliação da capacidade de carga do solo reforçado com geogrelha natural. In *Anais do 12º Simpósio de Práticas de Engenharia Geotécnica da Região Sul*, Joinville, SC. São Paulo: ABMS.
- Maccaferri. (2019). *Catálogo de especificações técnicas: microgrelha MacGrid®* (Documento interno). Maccaferri do Brasil Ltda.
- Palmeira, E.M. (2018). *Geossintéticos em geotecnia e meio ambiente*. São Paulo: Oficina de Textos.
- Pinto, C.D.S. (2006). *Basic course in soil mechanics* (3rd ed.). São Paulo: Oficina de Textos.
- Santos, C.E.D., Guedes, E.D.S.R., Rocha, E.D.P.L., Lima, G.P.L., Moura, G.D.J., Santos, I.S.D., Barros, J.H.M., & Santos, M.L.D.J. (2021). Capacidade de carga de solo reforçado com geossintéticos. *Brazilian Journal of Development*, 7(1), 11558-11579. <https://doi.org/10.34117/bjdv7n1-788>.
- Sharma, R., Chen, Q., Abu-Farsakh, M., & Yoon, S. (2009). Analytical modeling of geogrid reinforced soil foundation. *Geotextiles and Geomembranes*, 27(1), 63-72. <https://doi.org/10.1016/j.geotexmem.2008.07.002>.
- Teixeira, A.H., & Godoy, N.S. (1998). Análise, projeto e execução de fundações rasas. In Hachich, W., Falconi, F.F., Saes, J.L., Frota, R.G.Q., Carvalho, C.S., & Niyama, S. (Eds.), *Fundações: teoria e prática* (2ª ed., pp. 227-264). São Paulo: Pini. (in Portuguese).
- Teles Júnior, R.C.B. (2022). *Caracterização mecânica de solos arenosos reforçados com microgrelha* [Master's dissertation, Federal University of Ceará]. Federal University of Ceará's repository (in Portuguese). Retrieved in November 9, 2024, from <https://www.repositorio.ufc.br/handle/riufc/66074>
- Teles Júnior, R.C.B., Soares, A.B., & Aguiar, M.F.P. (2025). Drained tests on sandy soils reinforced with microgrids. *Soils and Rocks*, 48(1), e2025003222. <https://doi.org/10.28927/SR.2025.003222>.